Self-noise cancellation methods applied to acoustic underwater sensors

ALEX CEDERHOLM, MATTIAS JÖNSSON

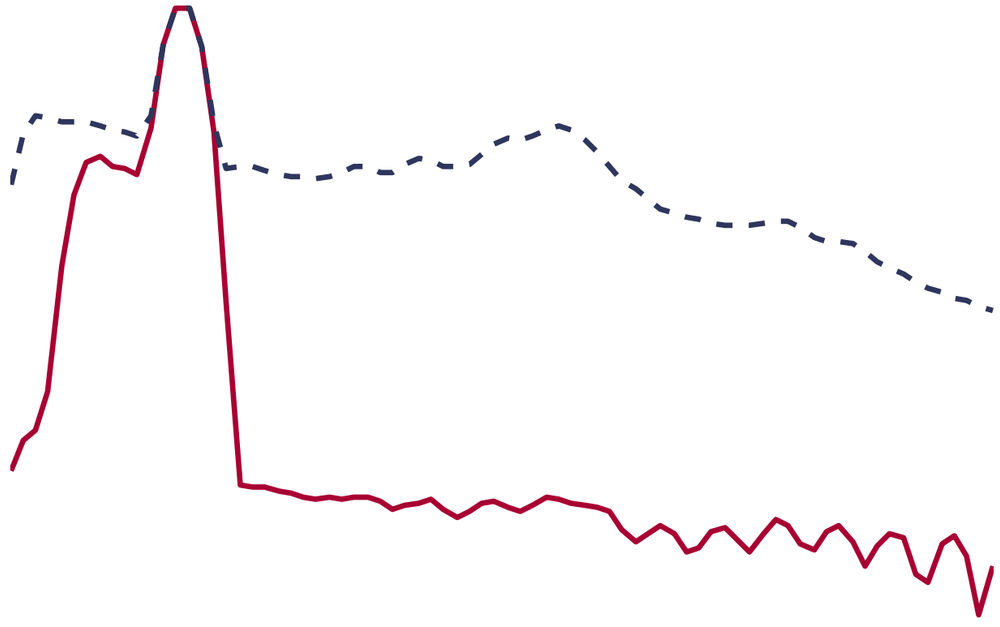

FOI, Swedish Defence Research Agency, is a mainly assignment-funded agency under the Ministry of Defence. The core activities are research, method and technology development, as well as studies conducted in the interests of Swedish defence and the safety and security of society. The organisation employs approximately 1000 personnel of whom about 800 are scientists. This makes FOI Sweden's largest research institute. FOI gives its customers access to leading-edge expertise in a large number of fields such as security policy studies, defence and security related analyses, the assessment of various types of threat, systems for control and management of crises, protection against and management of hazardous substances, IT security and the potential offered by new sensors.

FOI
Defence Research Agency
Defence & Security, Systems and Technology
SE-164 90 Stockholm

Phone: +46 8 555 030 00
Fax: +46 8 555 031 00

www.foi.se

FOI-R--2573--SE Technical report
ISSN 1650-1942 October 2008

Defence & Security, Systems and Technology

Alex Cederholm, Mattias Jönsson

Self-noise cancellation methods applied to acoustic underwater sensors

Titel	Metoder för egenbullerundertryckning tillämpat på akustiska undervattenssensorer
Title	Self-noise cancellation methods applied to acoustic underwater sensors
Rapportnr/Report no	FOI-R--2573--SE
Rapporttyp Report Type	Teknisk rapport Technical report
Sidor/Pages	28 p
Månad/Month	Oktober/October
Utgivningsår/Year	2008
ISSN	ISSN 1650-1942
Kund/Customer	Försvarsmakten
Forskningsområde Programme area	4. Sensorer och signaturanpassning 4. Sensors and Low Observables
Delområde Subcategory	43 UV-teknik – sensorer 43 Underwater Technology - Surveillance, Target acquisition and Reconnaissance
Projektnr/Project no	E20608
Godkänd av/Approved by	Helena Bergman

FOI, Totalförsvarets Forskningsinstitut
Avdelningen för Försvars- och säkerhetssystem
164 90 Stockholm

FOI, Swedish Defence Research Agency
Defence & Security, Systems and Technology
SE-164 90 Stockholm

Sammanfattning

Spaningsplattformars egenbuller kan kategoriseras i utrustnings- och plattformsbuller. Utrustningsbuller karakteriseras av momentana förlopp och är inte knuten till själva spaningen, t.ex. buller producerat av rörledningar. Buller från sensorplattformen inkluderar maskin- och hydrodynamiska ljud som orsakas av farkostens rörelser i vattnet. Reduktion av den negativa påverkan som egenbuller har på spaningsprestanda angrips utifrån ett signalbehandlingsperspektiv. Två lovande bullerundertryckningsmetoder studeras, där båda metoderna uppskattar bullret och sedan sker en filtrering. Den första metoden estimerar bullret genom anpassning till en AR (jmf. eng. AutoRegressive) modell, medan den andra metoden använder en ICA (jmf. eng. Independent Component Analysis) metod. Sedan görs en filtrering med hjälp av ett FIR (jmf. eng. Finite Impulse Response) Wiener filter samt tre olika adaptiva FIR filter: LMS, NLMS och RLS. Metoderna tillämpas på signaler registrerade med en TAS (jmf. eng. Towed Array Sonar), tagna från ett fältförsök som genomförts i Stockholms skärgård. AR-metoden fungerar tillfredställande och undertrycker buller med 30 dB/Hz oberoende av vilket filter som används och även om korrelationskoefficienten mellan störning och uppmätt buller är så låg som 0.2. ICA metoden reducerar bullret med 10 dB/Hz i det frekvensband där egenbullret återfinns oberoende av vilket filter som används.

Nyckelord: Egenbullerundertryckning, Passiv sonar, TAS, ICA, AR process, Filter, Wiener, LMS, NLMS, RLS

Summary

Self-noise generating mechanisms can be categorised in noise produced by the equipment and the platform. Equipment noise has characteristics of being instantaneous in nature, e.g. transients such as tube noise. The noise produced by the sensor platform includes noise from the machinery and hydrodynamic noise generated by the motion of the platform in the water. A signal processing perspective on reducing the negative impact of self-noise is taken. Two promising self-noise cancellation methods are investigated. Both methods consist of a noise estimation followed by filtering. The first method estimates the noise by fitting an AutoRegressive (AR) model, while the second approach uses an Independent Component Analysis (ICA) method. A Finite Impulse Response (FIR) Wiener filter and three different adaptive FIR filters, LMS, NLMS and RLS are then applied. The methods are applied to Towed Array Sonar (TAS) signals taken from a field test carried out in the archipelago of Stockholm. The AR approach performs well regardless of which filter used and suppresses the noise by 30 dB/Hz even when the correlation coefficient between the interfering and measured noise is as low as 0.2. The ICA method reduces the noise in the main frequency band by 10 dB/Hz for all filters.

Keywords: Self-noise cancellation, Passive sonar, TAS, ICA, AR process, Filter, Wiener, LMS, NLMS, RLS

Contents

1 Introduction

Self-noise is a critical and complex aspect when considering the performance of sensor platforms. When using a sensor platform for underwater reconnaissance, e.g. sonar systems mounted on or towed by submarines and surface ships, it usually includes motion. The motion of the platform generates self-noise, which can degrade sonar performance. Presently in Sweden the self-noise is monitored in sonar systems of the Royal Swedish Navy (RSwN) and when possible measures are taken to prevent it. Attention should however also be directed to the understanding of the generating mechanism of a particular self-noise component in a sonar system. In addition, automatic tools for alerting of the presence of self-noise and reducing its impact on the sonar are important, and these tools will support the listening sonar operator in discriminating self-noise from ambient noise and targets. Thus, the challenge of monitoring and handling self-noise applies to the RSwN and is the motivation for the present study. The report will focus on reducing the impact of self-noise in sonar from a signal processing perspective.

Several mechanisms contribute to the self-noise and some strongly depend on the sensor platform itself [1]. Some general features and mechanisms of self-noise in sensors should still be mentioned. Sensor will here mean an array of hydrophone elements used for passive sonar. By different travel paths self-noise propagates as waves, and these waves are measured as signals in the sensor, adding to the target signals and degrading the sensor performance. One way of characterising these waves is by considering their contribution to the energy spectrum as a function of frequency. This contribution to the spectrum can be relatively stable and consist of either harmonic components, random distributions over a broad frequency region or a combination of both. In addition, the contribution changes as functions of time both in a small and large scale, e.g. instantaneous variation versus ageing effects of the platform. Self-noise can also have transient behaviour, occurring instantaneous with different echo durations. Furthermore the self-noise can reach a sensor through different propagation paths and exhibit strong directivity.

Self-noise generating mechanisms can be categorised in noise produced by the equipment and the platform, see for instance [2]. Equipment noise has characteristics of being more instantaneous in nature, e.g. transients, such as tube noise. The means of reducing them are challenging involving both robustness aspects and adaptive capabilities. The noise produced by the sensor platform includes noise from the machinery and hydrodynamic noise generated by the motion of the platform in the water. Machinery noise mainly originates from the propulsion of the platform and auxiliary machinery, and can consist of a combination of discrete harmonics and broad-band parts. The energy distribution is to some degree stable, but depends strongly on the speed of the platform. This noise can be monitored and can also be partly counteracted by introducing damping material in the propagation path between the generating noise source and the sensor. The ageing effects of machinery will however change the energy distribution of the noise over time and could make damping solutions less effective. Hydrodynamic noise mainly originates from flow-excited vibration, turbulence and cavitations, and can as machinery noise have both discrete and broader parts in their energy spectra. The type of noise also depends on the speed of the platform. This noise can be partly reduced by a careful design of the hull of the platform taking fluid mechanics aspects into account. Generally, the monitoring of self-noise is achieved by reference

sensors, such as accelerometers and hydrophones when applicable, which are placed at carefully selected locations on the platform.

As mentioned, self-noise can be anticipated and partly prevented in the construction phase of the platform. An alternative way is to consider the possibility to use signal processing to reduce the negative impact of self-noise in a sensor. As we have found in the literature, signal processing methods are rarely found, which apply to the reduction of self-noise for underwater reconnaissance platforms. However, some general comments can be made and in this context filtering using measured self-noise in the sensor is an obvious choice. As noise sources have different origins, filters either have to be adapted for each type of noise or a single filter has to be robust and able to handle different types of noise. One approach is to separate the self-noise from the wanted wavefield in the frequency-wavenumber domain, see [3] and [4]. In this way waves which have travelled with a speed different from the speed in water can be discriminated from the hydroacoustic waves. The importance of self-noise cancellation in sonar systems can be viewed from many different perspectives. From an operator viewpoint [5] several different display tools are crucial. As already mentioned, sonar systems in general are exposed to disturbances, among which self-noise can degrade performance [1]. This can be further emphasised by [6] with respect to beamforming and by [7] with respect to filtering, in particular Least Mean Squares (LMS). Furthermore, techniques from speech-recognition can be insightful, such as the Independent Component Analysis (ICA) for blind signal separation combined with adaptive noise cancelling found in [8].

We propose a combination of techniques which first assumes the noise to be an AutoRegressive (AR) process [9] or possibly to be decomposed by means of ICA [10]. This estimation requires a measurement without targets and varying the speed of the platform, enabling easier characterisation of the self-noise. It is also assumed that the properties of the ambient noise are a priori known or estimated. If measurements are carried out with targets directly, some a priori knowledge is needed regarding the properties of the ambient noise and either some features of the target signatures or some characteristics of the self-noise. The proposed combinations of methods can be seen as pre-processing of array signals before applying for instance beamforming.

The AR model may be used to model a random process [11]. Filtering white noise with a filter having p poles generates an $AR(p)$ random process. Carefully positioning of the poles using features of the signals generates the desired process. ICA is instead a class of statistical methods, which are utilised for transforming observed multidimensional data into components that are as statistically independent as possible. The a priori knowledge required is how many independent components should be searched for. In the literature several approaches for ICA can be found, see for instance the extensive tutorial in [10]. The linear ICA approach used in the present investigation follows the one found in [12]. It should be mentioned that the noise estimation techniques to some extent use contradictive assumptions, for instance Gaussian or non-Gaussian distributions, and different a priory knowledge, however this complies to the noise characteristics which may vary for different applications.

When the noise has been estimated by AR modelling or ICA, Finite Impulse Response (FIR) Wiener filtering techniques [11] are applied to the signals using the estimates. The Wiener filter is designed to be the optimum filter in recovering the desired signal from a noisy measurement. The filter is optimum in the sense that it minimises the mean square error. An assumption however requires the signals to be stationary, but the adaptive filters can be applied to non-stationary signals. The adaptive Least Mean Squares (LMS), Normalised

Least Mean Squares (NLMS) and Recursive Least Squares (RLS) FIR filters are also included in the study. Adaptive filters applied to the problem of noise cancellation is described in [13]. Experimental results for practical applications including electrocardiography, speech signals and antenna sidelobe interference are shown together with computer simulations of periodic or broadband interference where there is no external reference source. Here direct-form FIR filters are studied, the filters can however be implemented in other realizations and as Infinite Impulse Response (IIR) filters. An overview of adaptive IIR filtering is given in [14]. Two formulations: the equation-error and the output-error are described using a direct-form implementation, the parallel and lattice realizations are briefly discussed. A thorough review of the LMS filter applied to active noise control is found in [15].

The present analysis can be seen as an initial study of two promising self-noise cancellation methods taken from the vast number of possible methods found in signal processing research. Despite this fact, the methods have been tested on signals from field tests. A first attempt was made to apply the methods on signals taken from a field test involving an operative sensor platform of the RSwN. In this case sonar signals were registered both without and with targets. In addition, the speed of the sensor platform was varied enabling some discrimination of ambient-noise and self-noise. Unfortunately the signals were of poor quality due to malfunctions in the data acquisition equipment. The attention was instead directed to a field test where signals were registered with a Towed Array Sonar (TAS) of the RSwN, including self-noise, ambient noise and target at the same time [16]. The target was however a fixed source transmitting four tones, which simplifies the discrimination of the target signature. Nevertheless, the noise has to be estimated with the target present, which is a modification to the wanted prerequisites of the pre-processing and not the optimum choice. In addition, as the target consists of tones an obvious choice would be to process the data with a band-pass filter, but it is assumed that target information is not known a priori to comply with the self-noise cancellation methods proposed. Some recent progress in TAS research is reported in [1].

The structure of the report is as follows. In Chapter 2, brief explanations of noise cancellation filters and ICA are found. Then Chapter 3 starts with some information regarding the field test and the signals, which will be processed. This chapter also includes results from the AR, ICA and filter processing. The report ends with conclusions in Chapter 4, along with some comments regarding the next steps in the future development of self-noise cancellation methods.

2 Methods

2.1 Notations

In this chapter the investigated methods are briefly explained and some general notation rules are therefore required. The first and second derivative of a function of one variable $f(x)$ are indicated by $f'(x)$ and $f''(x)$. Matrices are written in bold capital letters ($\boldsymbol{A}$) while vectors are written in bold small letters ($\boldsymbol{x}$). Symbols for matrix operations are defined which are: $\boldsymbol{A}^T$, $\boldsymbol{A}^*$ and $\boldsymbol{A}^{-1}$ denoting the transpose, the conjugate and the inverse of a matrix respectively. The transpose and conjugate are also applicable on vectors. The null matrix is denoted by $\mathbf{0}$.

Let $\boldsymbol{x} = [x_1, ..., x_N]^T$ be a vector with dimension N. The expectation value of $\boldsymbol{x}$ is denoted by $E\{\boldsymbol{x}\} \approx m_x$ and estimates its sample mean $m_x = \frac{1}{N}\sum_{i=1}^{N} x_i$. The expectation value of a matrix can be written as $E\{\boldsymbol{X}\} \approx \boldsymbol{m}_x$ and is a column vector with N components, where each n^{th} component equals the mean of the corresponding row n. The matrix $\tilde{\boldsymbol{X}} = \boldsymbol{X} - \boldsymbol{m}_x$ is defined to be centred as $E\{\tilde{\boldsymbol{X}}\} = \mathbf{0}$. To apply whitening/sphering on $\boldsymbol{X}$ an eigenvalue decomposition of its covariance matrix $\boldsymbol{R}_x = E\{\boldsymbol{X}\boldsymbol{X}^T\}$ is required. Assuming that the eigenvalue decomposition of the covariance matrix can be written in the following form $\boldsymbol{R}_x = \boldsymbol{E}\boldsymbol{D}\boldsymbol{E}^T$, a change of coordinates to $\tilde{\boldsymbol{X}} = \boldsymbol{E}\boldsymbol{D}^{-1/2}\boldsymbol{E}^T\boldsymbol{X}$ will result in $\tilde{\boldsymbol{X}}$ being whitened, i.e. $E\{\tilde{\boldsymbol{X}}\tilde{\boldsymbol{X}}^T\} = \boldsymbol{I}$. If a vector $\boldsymbol{x}$ or a matrix $\boldsymbol{X}$ are estimated, the estimations are denoted by $\hat{\boldsymbol{x}}$ and $\hat{\boldsymbol{X}}$ respectively. A p^{th} order FIR filter W is denoted by its system function $W(z) = \sum_{l=0}^{p-1} w(l)z^{-l}$ or the impulse response vector $\boldsymbol{w} = [w(0), w(1), \ldots, w(p-1)]^T$. The adaptive filter coefficients at time n is denoted by $\boldsymbol{w}_n = [w(0)_n, w(1)_n, \ldots, w(p-1)_n]^T$.

2.2 Noise cancellation filters

Assume that an observation x of a desired signal d is interfered by additive noise v_1 as follows,

$$x(n) = d(n) + v_1(n) \ . \tag{2.1}$$

The noise is also measured by a reference sensor v_2, where v_2 is not equal to v_1 but correlated to it [11]. From v_2, v_1 is estimated, $\hat{v}_1$, using a filter $W(z)$. The desired signal is then estimated as,

$$\hat{d}(n) = x(n) - \hat{v}_1(n) \ . \tag{2.2}$$

Thus the noise can be decreased if v_1 can be determined from v_2. Using this system the task of removing the noise v_1 is merely determining the filter $W(z)$. The remainder of this section will describe different methods to estimate v_1 from v_2 following [11].

2.2.1 FIR Wiener filter

A Wiener filter is an optimum filter minimising the mean square error ξ as,

$$\xi(n) = E\left\{|e(n)|^2\right\} = E\left\{\left|d(n) - \hat{d}(n)\right|^2\right\} \ . \tag{2.3}$$

Consider a p^{th} order FIR filter,

$$W(z) = \sum_{l=0}^{p-1} w(l) z^{-l} \ . \tag{2.4}$$

The error can then be written as,

$$e(n) = d(n) - \left(x(n) - \sum_{l=0}^{p-1} w(l) v_2(n-l) \right) \ . \tag{2.5}$$

The optimum filter coefficients, $w(k)$, is found by setting the derivative of ξ with respect to $w^*(k)$ equal to zero for $k = 0, 1, \ldots, p-1$. This yields,

$$E\left\{ e(n) v_2^*(n-k) \right\} = 0, \ k = 0, 1, \ldots, p-1 \ . \tag{2.6}$$

Using equation (2.5) in (2.6) and assuming that v_2 is uncorrelated with d gives the Wiener-Hopf equations,

$$\sum_{l=0}^{p-1} w(l) r_{v_2}(k-l) = r_{xv_2}(k), \ k = 0, 1, \ldots, p-1 \ , \tag{2.7}$$

where $r_{v_2}(k) = E\left\{ v_2(n) v_2^*(n-k) \right\}$ is the autocorrelation of v_2 and $r_{xv_2}(k) = E\left\{ x(n) v_2^*(n-k) \right\}$ is the cross-correlation between x and v_2. Introducing the matrix of autocorrelations,

$$\boldsymbol{R}_{v_2} = \begin{bmatrix} r_{v_2}(0) & r_{v_2}^*(1) & \ldots & r_{v_2}^*(p-1) \\ r_{v_2}(1) & r_{v_2}(0) & \ldots & r_{v_2}^*(p-2) \\ \vdots & \vdots & & \vdots \\ r_{v_2}(p-1) & r_{v_2}(p-2) & \ldots & r_{v_2}(0) \end{bmatrix} \tag{2.8}$$

the Wiener-Hopf equations can be written in matrix form,

$$\boldsymbol{R}_{v_2} \boldsymbol{w} = \boldsymbol{r}_{xv_2} \ , \tag{2.9}$$

where $\boldsymbol{w} = [w(0), w(1) \ldots w(p-1)]^T$ and $\boldsymbol{r}_{xv_2} = [r_{xv_2}(0), r_{xv_2}(1), \ldots r_{xv_2}(p-1)]^T$. The Wiener filter requires the autocorrelation and cross correlation to be known or estimated. Furthermore d, v_1 and v_2 are assumed to be wide-sense stationary.

2.2.2 LMS - Least Mean Squares

Consider an adaptive p^{th} order FIR filter where the filter coefficients are continuously updated as follows,

$$\boldsymbol{w}_{n+1} = [w(0)_{n+1}, w(1)_{n+1}, \cdots, w(p-1)_{n+1}]^T = \boldsymbol{w}_n + \boldsymbol{\Delta w}_n \ . \tag{2.10}$$

Let $\boldsymbol{w}_n$ be an estimate minimising the quadratic mean square error function in equation (2.3). Using the method of steepest descent $\boldsymbol{w}_n$ is updated by taking a step of size μ in the direction of maximum descent down the error surface as,

$$\boldsymbol{w}_{n+1} = \boldsymbol{w}_n - \mu \nabla \xi(n) \ , \tag{2.11}$$

where ∇ denotes the gradient. The derivative of ξ with respect to $\boldsymbol{w}^*$ yields,

$$\nabla \xi(n) = -E\left\{ e(n) \boldsymbol{v}_2^*(n) \right\} \ . \tag{2.12}$$

The expectation in equation (2.12) can be estimated by the sample mean as,

$$\hat{E}\left\{e(n)\boldsymbol{v}_2^*(n)\right\} = \frac{1}{L}\sum_{l=0}^{L-1} e(n-l)\boldsymbol{v}_2^*(n-l) \ . \tag{2.13}$$

Equations (2.11) and (2.13) with $(L = 1)$ yields the LMS algorithm,

$$\boldsymbol{w}_{n+1} = \boldsymbol{w}_n + \mu e(n)\boldsymbol{v}_2^*(n) \ . \tag{2.14}$$

The LMS algorithm converges in the mean to the optimum filter $\boldsymbol{w}$ if

$$0 < \mu < \frac{2}{\lambda_{max}} \ , \tag{2.15}$$

where λ_{max} is the largest eigenvalue of the autocorrelation matrix $\boldsymbol{R}_{v_2}$. The autocorrelation is required to be known or estimated if convergence in the mean is to be guaranteed. Compared to the Wiener filter, the LMS filter coefficients are time dependent allowing d, v_1 and v_2 to be nonstationary.

2.2.3 NLMS - Normalised Least Mean Squares

By introducing the normalised step size,

$$\beta = \frac{\mu}{\left\|\boldsymbol{v}_2(n)\right\|^2} \ , \tag{2.16}$$

into the LMS algorithm (2.14) yields the NLMS algorithm,

$$\boldsymbol{w}_{n+1} = \boldsymbol{w}_n + \beta\frac{\boldsymbol{v}_2^*(n)}{\epsilon + \left\|\boldsymbol{v}_2(n)\right\|^2}e(n) \ , \tag{2.17}$$

where ϵ is some small positive number. The NLMS algorithm converges in the mean to the optimum filter $\boldsymbol{w}$ if

$$0 < \beta < 2 \ . \tag{2.18}$$

The NLMS algorithm requires no correlation matrices and d, v_1 and v_2 are allowed to be nonstationary.

2.2.4 RLS - Recursive Least Squares

Consider the exponentially weighted least squares error,

$$\zeta(n) = \sum_{i=0}^{n} \lambda^{n-i}\left|e(i)\right|^2 = \sum_{i=0}^{n} \lambda^{n-i}\left|d(i) - \hat{d}(i)\right|^2 \ , \tag{2.19}$$

where the forgetting factor λ is $0 < \lambda \leq 1$. An adaptive FIR filter,

$$\boldsymbol{w}_{n+1} = \left[w(0)_{n+1}, w(1)_{n+1}, \cdots, w(p-1)_{n+1}\right]^T = \boldsymbol{w}_n + \boldsymbol{\Delta w}_n \ , \tag{2.20}$$

yields the following error,

$$e(i) = d(i) - \left(x(i) - \sum_{l=0}^{p-1} w(l)v_2(i-l)\right) \ . \tag{2.21}$$

The optimum filter coefficients, $\boldsymbol{w}_n$, minimising the least squares error is found by setting the derivative of ζ with respect to $w_n^*(k)$ equal to zero for $k = 0, 1, \ldots, p-1$. This yields,

$$\sum_{i=0}^{n} \lambda^{n-i} e(i)v_2^*(i-k) = 0, \ k = 0, 1, \ldots, p-1 \ . \tag{2.22}$$

Introducing the data vector $\boldsymbol{v}_2(i) = [v_2(i), v_2(i-1), \cdots, v_2(i-p)]^T$ and using equation (2.21) in (2.22) gives the deterministic normal equations,

$$\boldsymbol{R}_{v_2}(n)\boldsymbol{w}_n = \boldsymbol{r}_{xv_2}(n) \ , \tag{2.23}$$

where $\boldsymbol{R}_{v_2}(n)$ is the exponentially weighted deterministic autocorrelation matrix at time n,

$$\boldsymbol{R}_{v_2}(n) = \sum_{i=0}^{n} \lambda^{n-i} \boldsymbol{v}_2^*(i)\boldsymbol{v}_2^T(i) \ , \tag{2.24}$$

and $\boldsymbol{r}_{xv_2}(n)$ is the exponentially weighted deterministic cross-correlation between x and v_2,

$$\boldsymbol{r}_{xv_2}(n) = \sum_{i=0}^{n} \lambda^{n-1} x(i)\boldsymbol{v}_2^*(i) \ . \tag{2.25}$$

Notice that the correlations may be determined recursively in the following way,

$$\boldsymbol{R}_{v_2}(n) = \lambda \boldsymbol{R}_{v_2}(n-1) + \boldsymbol{v}_2^*(n)\boldsymbol{v}_2^T(n) \ , \tag{2.26}$$

$$\boldsymbol{r}_{xv_2}(n) = \lambda \boldsymbol{r}_{xv_2}(n-1) + x(n)\boldsymbol{v}_2^*(n) \ . \tag{2.27}$$

Let $\boldsymbol{P}(n) = \boldsymbol{R}_x^{-1}(n)$ denote the inverse of the autocorrelation matrix at time n. Applying Woodbury's identity [17] the inverse of the autocorrelation matrix can recursively be updated,

$$\boldsymbol{P}(n) = \lambda^{-1}\left[\boldsymbol{P}(n-1) - \boldsymbol{g}(n)\boldsymbol{v}_2^T(n)\boldsymbol{P}(n-1)\right] \ , \tag{2.28}$$

where

$$\boldsymbol{g}(n) = \frac{\lambda^{-1}\boldsymbol{P}(n-1)\boldsymbol{v}_2^*(n)}{1 + \lambda^{-1}\boldsymbol{v}_2^T(n)\boldsymbol{P}(n-1)\boldsymbol{v}_2^*(n)} \ . \tag{2.29}$$

The recursive solution to (2.23) is then,

$$\boldsymbol{w}_n = \boldsymbol{w}_{n-1} + \alpha(n)\boldsymbol{g}(n) \ , \tag{2.30}$$

where

$$\alpha(n) = x(n) - \boldsymbol{w}_{n-1}^T\boldsymbol{v}_2(n) \ . \tag{2.31}$$

Since the RLS algorithm minimises the least squares error instead of the mean square error no statistical information needs to be estimated and correlation matrices may be computed from the data. Furthermore the deterministic approach of adapting the filter coefficients to the instantaneous signals removes any constraint on stationary signals. In fact two signals from the same random process will produce two different filters.

2.3 ICA - Independent Component Analysis

ICA is utilised for transforming observed multidimensional data into components that are as statistically independent as possible. The linear ICA approach used in the present investigation follows the one found in [12]. Here the theory behind the approach is repeated and put into context with respect to the application, measuring target signals with a hydrophone array and where noise from the sensor platform interfere the signals.

Let data be gathered in a matrix $\boldsymbol{X}$ with dimensions $(N \times M)$. For time-series data registered with an array the dimension N denotes the number of sensor elements and the dimension M denotes the number of instantaneous time samples of the signal. Let in addition instantaneous samples of observed time-series data in N sensor elements be gathered in a column vector $\boldsymbol{x} = [x_1, ..., x_N]^T$ and assume that the signals consist of a mixture of statistically mutually independent components $\boldsymbol{s} = [s_1, ..., s_N]^T$ with non-Gaussian probability distributions. The components of $\boldsymbol{s}$ could be seen as signals originating from target signals or noise sources. The data $\boldsymbol{x}$ could for instance consist of registered signals in N hydrophone elements of a TAS at a fixed instantaneous time $x(t_i) = x_i$. The ICA problem can be formulated as estimating a weight matrix $\boldsymbol{W}$ resulting in a linear transformation of the observed data $\boldsymbol{x}$ [12],

$$\boldsymbol{s} = \boldsymbol{W}\boldsymbol{x} \ . \tag{2.32}$$

The transformation of equation (2.32) should result in the components s_i being as statistically independent as possible. An alternative is to consider the following mixing model [12],

$$\boldsymbol{x} = \boldsymbol{A}\boldsymbol{s} \ , \tag{2.33}$$

and where $\boldsymbol{A}$ denotes the mixing matrix. As can be seen in equations (2.32) and (2.33) the matrix $\boldsymbol{W}$ is obtained by the estimated inverse of the mixing matrix, $\boldsymbol{A}^{-1}$.

Having stated the starting point of ICA in equation (2.33), consider a linear combination of x_i weighted with a column vector $\boldsymbol{w} = [w_1, ..., w_N]^T$ as $y = \boldsymbol{w}^T\boldsymbol{x}$. The vector $\boldsymbol{w}$ should now be determined. If $\boldsymbol{w}$ would equal the i^{th} row of $\boldsymbol{A}^{-1}$ with $i \in [1, ..., N]$, the resulting linear combination will result in $y = s_i$. The question is how to find an estimator of $\boldsymbol{w}$ which approximates one of the rows of $\boldsymbol{A}^{-1}$. By introducing the variables $\boldsymbol{z} = \boldsymbol{A}^T\boldsymbol{w}$, i.e. a coordinate transformation, the linear combination y can be written as $y = \boldsymbol{w}^T\boldsymbol{x} = \boldsymbol{w}^T\boldsymbol{A}\boldsymbol{s} = \boldsymbol{z}^T\boldsymbol{s}$. This results in y being a linear combination of the independent component s_i with weights given by z_i. The idea of ICA is that the sum of independent random variables tends to be more Gaussian compared with the original variables and $y = \boldsymbol{z}^T\boldsymbol{s}$ is least Gaussian when only one element z_i in $\boldsymbol{z}$ is nonzero. Thus by maximising the non-Gaussianity of y, one independent component can be obtained $\pm s_i$. It turns out that the sign of the optimum is undetermined due to the optimisation landscape of y having two local maxima. In addition, the ambiguities of the present ICA approach will include no possibility to determine the variances and the order of the independent components [12].

Thus, the non-Gaussianity of y should be maximised. An information-theoretic measure of independence between random variables is the mutual information, however there exists other measures as well. It can be shown [12] that finding an invertible transformation of $\boldsymbol{W}$ that minimises the mutual information is roughly equivalent to finding directions in which the negentropy is maximised. The negentropy can be defined by normalising the differential entropy [12].

An estimate of the negentropy is required, i.e. an objective (contrast) function, where the sum of the negentropies of the components should be maximised. The choice of the objective function depends on consistency, asymptotic variance and robustness, as well as practical considerations such as computation complexity and processing time requirements [12]. It can be shown that

maximising the negentropy is approximately equivalent to search for the maximum of the following object function $E\{G_i(y)\}$. The functions $G_i(y)$ should be selected with care and here are some candidates [12],

$$\begin{aligned} G_1(y) &= \frac{1}{4}y^4 \ , \\ G_2(y) &= \frac{1}{a_1}\ln\{\cosh(a_1 y)\} \ , \\ G_3(y) &= -\frac{1}{a_2}\exp\{\frac{a_2 y^2}{2}\} \ , \end{aligned} \tag{2.34}$$

where a_1 and a_2 are constants. The choice of $G_i(y)$ is most important for optimising the ICA method itself.

Algorithms are suggested for the required maximisation of $E\{G_i(y)\}$, the fixed-point ICA algorithm for one unit along with a deflation scheme to handle several independent components [12]. The investigated data is denoted by $\boldsymbol{X}$ with dimensions according to the previously mentioned notations. Before the algorithm is applied to $\boldsymbol{X}$, pre-processing is performed by centring and if applicable $\boldsymbol{X}$ is whitened, i.e. a subspace is selected of dimensionality $P < N$. Firstly, let weight vectors $\boldsymbol{w}_p$ be gathered in a matrix $\boldsymbol{W}$. The p index denotes the p^{th} independent component of a total of P number of independent components searched for. The suggested algorithm follows the steps below.

i) Initialise $\boldsymbol{W} = \boldsymbol{0}$

ii) Select an initial random weight vector $\boldsymbol{w}_p$

iii) Apply decorrelation and normalisation to $\boldsymbol{w}_p$

iv) Check a convergence criterion
If the convergence criterion is fulfilled gather $\boldsymbol{w}_p$ in the p^{th} column of $\{\boldsymbol{W}\}_p$ and repeat from step *ii*) with the next independent component $\boldsymbol{w}_{p+1}$.
If the convergence criterion is not fulfilled continue to step *v*).

v) Let $\boldsymbol{w}_p^\dagger = E\{\boldsymbol{X}G_i'(\boldsymbol{X}^T\boldsymbol{w}_p)\} - E\{G_i''(\boldsymbol{X}^T\boldsymbol{w}_p)\}\boldsymbol{w}_p$

vi) Normalise $\boldsymbol{w}_p^\dagger$, set $\boldsymbol{w}_p = \boldsymbol{w}_p^\dagger$ and continue from step *iii*).

The deflation scheme (decorrelation) in step *iii*) can be written as

$$\boldsymbol{w}_{new} = \boldsymbol{w}_{old} - \boldsymbol{W}\boldsymbol{W}^T\boldsymbol{w}_{old} \ , \tag{2.35}$$

and the normalisation of weight vectors found in steps *iii*) and *vi*) are given by the standard 2-norm. In addition, the convergence criterion in step *iv*) is fulfilled if $||\boldsymbol{w}_{new} - \boldsymbol{w}_{old}|| < \epsilon$ and $||\boldsymbol{w}_{new} + \boldsymbol{w}_{old}|| < \epsilon$ are reached, where ϵ is an appropriately selected small number. The step *v*) above is derived from conditions stated in [12] along with finding an optimum utilising Newton's method. In practice, the expectation values found in the algorithm is replaced by estimates using the corresponding sample means.

By selecting the number of independent components searched for with care, the ICA processing in the array case will produce a set of independent signals. The choice of the number of independent components depends on several aspects, such as number of targets, target signature, self-noise and ambient noise. In the present study, ICA is used to suggest an estimation of the noise in the measured signals and then this estimate is used in the noise cancellation filters previously explained.

3 Results

3.1 Experimental data

The described methods in Chapter 2 are applied to experimental data taken from a field test [16]. This field test was carried out in the archipelago of Stockholm, where the underwater environment was typical of the shallow waters found in the Baltic Sea. With a fixed transmitter signals were registered with a TAS. The source transmitted tones (sinusoids) at four different frequencies 80, 93, 121 and 173 Hz. The measured signals are expected to contain both ambient- and self-noise, which can degrade the performance of the TAS. The sensor platform is considered to encompass both the TAS and the towing surface ship, and thus the self-noise can be assumed to originate firstly from the ship, e.g. machinery and hydrodynamic noise. Secondly the motion of the TAS will induce flow noise, most likely being turbulence, which adds to the self-noise energy in the signals. As previously mentioned in Chapter 1, self-noise in general is a critical and complex issue, and it can originate from several different mechanisms [2]. To characterise the noise sources is however not the main focus of the study, instead it is the presence of noise in the signals and the ability of the proposed methods to reduce the noise that is of importance here.

The tracks of the ship towing the TAS consisted of a straight leg followed by a sharp turn and then this motion was repeated several times. The straight legs of the tracks were approximately perpendicular to the direction of propagation from the source to the center of the straight track. If only the transmitted energy from the source is considered, the received energy in the TAS will vary in bearing as a function of time. The sharp turn will instead mainly result in the TAS receiving energy from a constant bearing, while in addition being curved. Furthermore, the turn will probably produce additional self-noise and also introducing difficulties with the TAS being end-fire to the source degrading the resolution. Data from a straight track was selected for the analysis, and the TAS was approximated with a linear array. Data was taken with a sampling frequency of 3333 Hz and encompassed 32 sensor elements of the TAS.

In Figure 3.1, a Bearing Time Record (BTR) is found for which signals have been processed with Conventional Beamforming (CB). Two channels have been excluded as they showed a different spectrum in comparison to the remaining channels. The diagram has been produced with CB in the frequency domain using a time step of 5 s and a window length of approximately 0.3 s. In the frequency synthesis, data between 60 and 1000 Hz have been processed, which includes the tones transmitted by the source, and without any further tampering of data. As can be seen in Figure 3.1 there is one completely dominating target, originating from the transmitted tones of the source, and the bearing of this track is varying with time as expected.

In Figure 3.2, the time series of sensor 30 is displayed, taken from the starting phase of the measurement. The characteristics of the signal are fairly typical for this data set. Looking into more details of the signals, in particular Power Spectral Density (PSD) estimates in Figure 3.2, the tones from the source can easily be discriminated and are fairly strong in comparison to the noise. The corresponding normalised PSD estimate in Figure 3.2 is based on approximately 2.5 s of data. The PSD has been calculated using a Welch spectral estimator and a segment length of 200 samples. A Chebyshev tapering

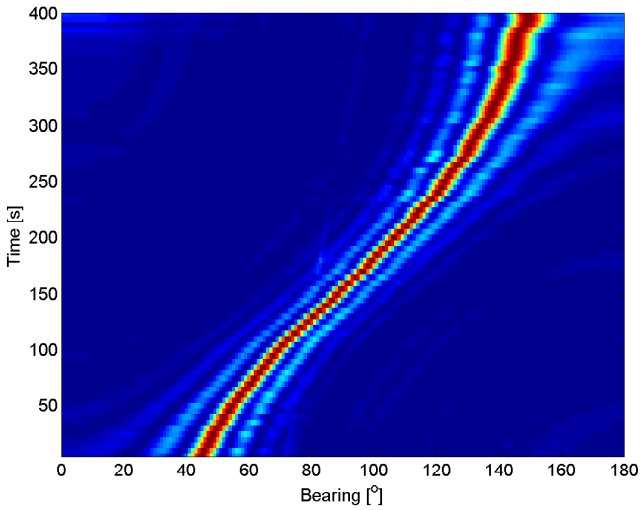

Figure 3.1: Resulting BTR when the signal data has been processed with a conventional frequency beamformer and selecting frequencies between 60 and 1000 Hz. The signals were processed with a 5 s time step and a window length of approximately 0.3 s.

window is used with a side-lobe attenuation of 80 dB and overlap of 30%. With a segment length of 200 and an overlap of 30%, enough averages are made to reduce the variance of the spectrum. Thus the focus is on amplitudes/levels rather than resolution, i.e. in this study the characteristics of possible ambient- and self-noise are of less importance. As can be seen in the PDS of Figure 3.2 the tones are dominating around 200 Hz, however only one peak is present due to the reduction of variance in the spectrum. Thus, this indicates that the data is well suited for the proposed filtering processes proposed. The setting of the PSD estimate used in Figure 3.2 will hereafter be used for all remaining PSD estimates presented, only varying in respect to using normalised amplitudes or dB-levels.

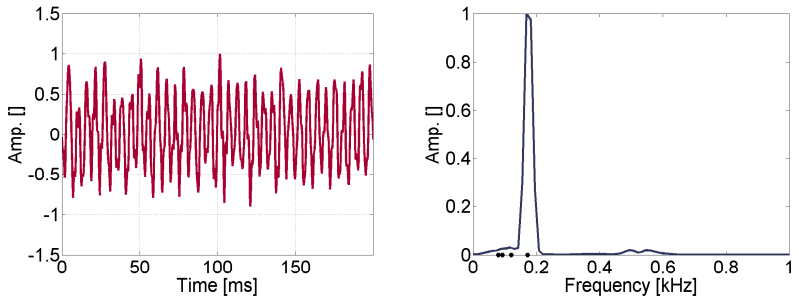

Figure 3.2: Left - Normalised signal as function of time for channel 30, taken from the starting phase of the measurement. Right - Normalised PSD estimate of the time signal using approximately 2.5 s of data. Black dots indicate the frequencies of the tones.

3.2 Wiener filter processing

In this section the performance of the noise cancellation filters, Wiener filter, LMS, NLM and RLS will be studied. The experimental data consists of signals from 32 TAS elements and here the arbitrary selected channel 11 will be studied. Since no reference measurement of the noise, i.e. ambient- and self-noise, is available the interfering noise has to be estimated. Note that the following estimation is only possible because the desired signal is simple and known. Normally this will not be the case and the noise should be measured. However for the purpose of evaluating the noise cancellation filters it is applicable. First the four sinusoids transmitted by the source are identified in the Fourier spectra. The noise is estimated using interpolation at the frequency bins occupied by the tones. The estimated noise time series will from now on be denoted by $\hat{v}_1$. Now assume that the noise could be modelled as an AR process. Thus the noise could be generated by filtering unit variance noise, g with an all-pole filter, $A(z)$. Using the Yule-Walker method [11] a 50^{th} order AR model was estimated from $\hat{v}_1$. Finally the unit variance noise $\hat{g}$ was determined from the estimated model and the noise Fourier spectra.

In Figure 3.3 the PSD estimates are shown for the data before and after filtering with the four different noise cancellation filters. The order of all filters where set to 6 and $\hat{v}_1$ was used as the reference noise. All filters performs well and a Signal-to-Noise Ratio (SNR) gain at about 40 dB/Hz is observed.

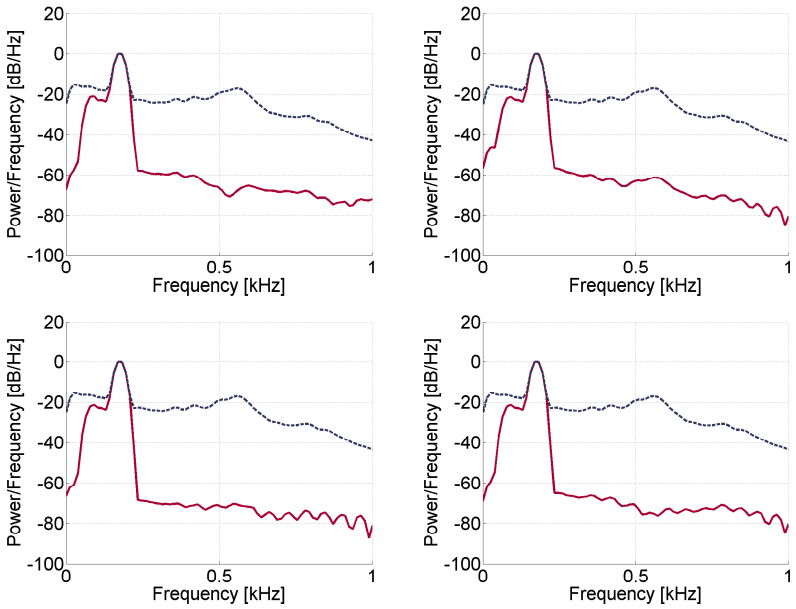

Figure 3.3: PSD estimates using measured signals before (blue dashed line) and after (red line) filtering with a 6^{th} order noise cancellation filter and estimating noise with an AR model. Wiener (top left), LMS (top right), NLMS (bottom left) and RLS (bottom right). See Figure 3.2 for details regarding the PSD settings.

Additional PSD estimates of the data and the result after filtering with the four different noise cancellation filters are shown in Figure 3.4. The order of all filters where 200 and $\hat{g}$ was used as the reference noise. The correlation coefficient between $\hat{g}$ and $\hat{v}_1$ was 0.2. Still all filters produce similar results as above and a SNR gain at about 40 dB/Hz is observed.

The experimental data has a high SNR. To evaluate performance at different

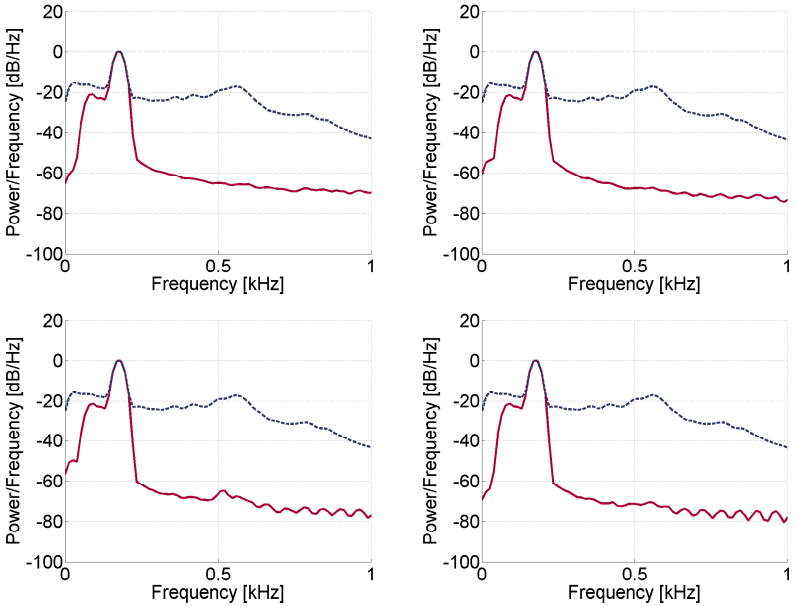

Figure 3.4: PSD estimates using measured signals before (blue dashed line) and after (red line) filtering with a 200$^{\text{th}}$ order noise cancellation filter and estimating noise with an AR model. Wiener (top left), LMS (top right), NLMS (bottom left) and RLS (bottom right). See Figure 3.2 for details regarding the PSD settings.

SNR conditions, simulations have been carried out. First a low SNR setup is studied. The data consists of a single sinusoid corrupted by noise. The PSD estimates before and after noise cancellation are shown in Figure 3.5. The sinusoid not visible in the original data becomes prominent after filtering. An SNR gain at about 60 dB/Hz for Wiener, LMS and NLMS is observed and 70 dB/Hz is observed for RLS.

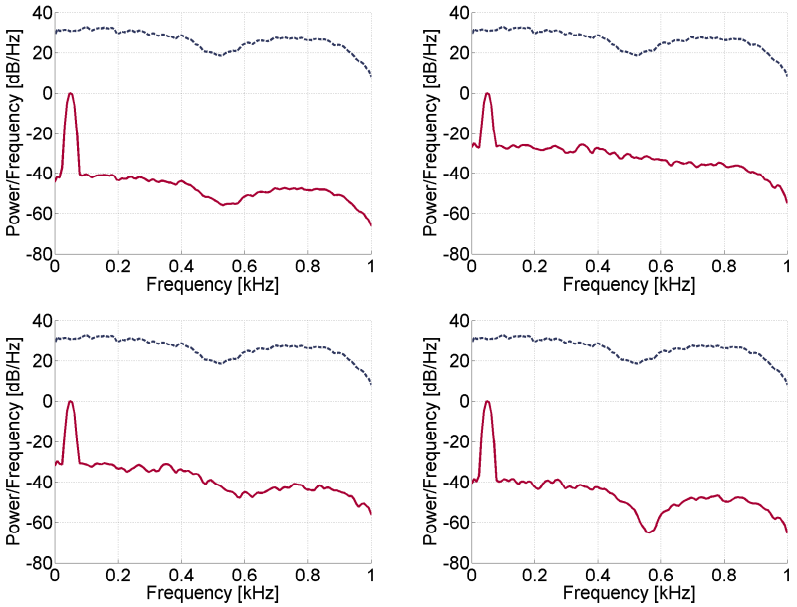

Figure 3.5: PSD estimates using simulated signals before (blue dashed line) and after (red line) filtering with Wiener (top left), LMS (top right), NLMS (bottom left) and RLS (bottom right). See Figure 3.2 for details regarding the PSD settings.

Examples of the LMS filter coefficients are shown in Figure 3.6. The coefficients converge after about 1000 samples to the correct value. All PSDs shown in this chapter are estimated using the output after the filters have converged.

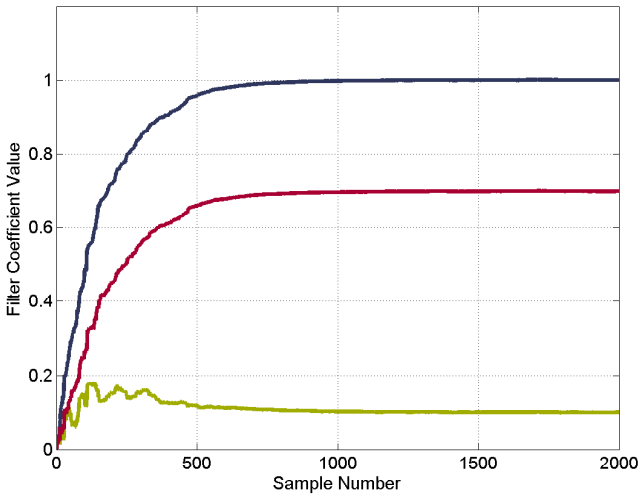

Figure 3.6: The estimated LMS filter coefficients from the simulation shown in Figure 3.5.

Figure 3.7 depicts the result from a simulation where the noise which interfere the observation is uncorrelated with the measured noise. The PSD estimates are shown for the observation, interfering noise, measured noise and result after Wiener filtering. As expected no improvement was achieved. When the interfering noise consists of contributions from different sources, e.g. different machinery parts, the different noise sources are likely to be uncorrelated. As seen in the previous simulation the measured noise has to be correlated with the corrupting noise to achieve any improvement.

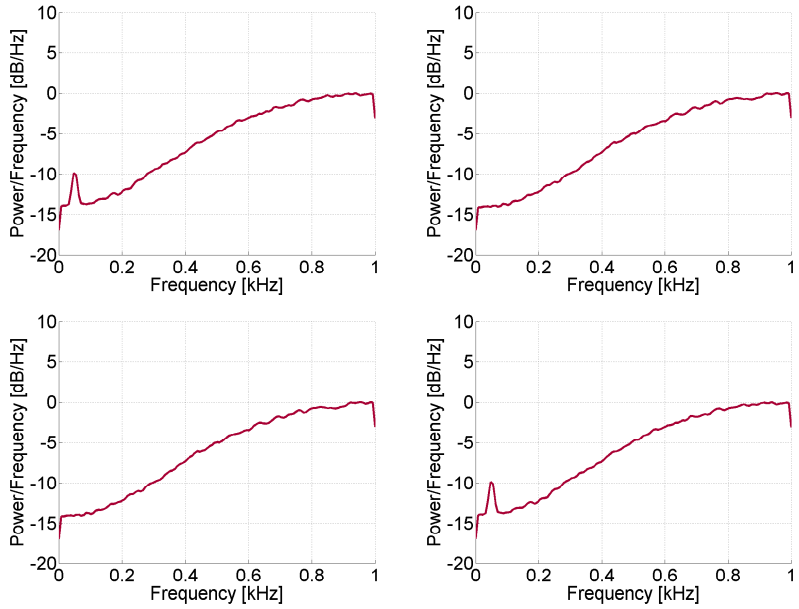

Figure 3.7: PSD estimates using simulated uncorrelated noise measured signal (top left), interfering noise (top right), measured noise (bottom left) and after Wiener filtering (bottom right). See Figure 3.2 for details regarding the PSD settings.

A simulation to test this situation has been performed. The total interfering noise in the observation of a sinusoid consists of the summation of three uncorrelated noise sources with different spectrum. A reference measurement of each individual noise source is available together with a reference measurement of the total noise. The situation is shown by PSD estimates in Figure 3.8 together with the result after noise cancellation with a Wiener filter. Both a single filter working with the reference measurement of the combined noise and three successive filters working with a measurement of each noise source were tested. The single filter achieves a SNR gain of about 10 dB/Hz and does not reveal the sinusoid. The test with three successive filters shows that the noise correlated to the measured noise is removed after each filter and the final result gives a SNR gain of about 60 dB/Hz with a very prominent sinusoid.

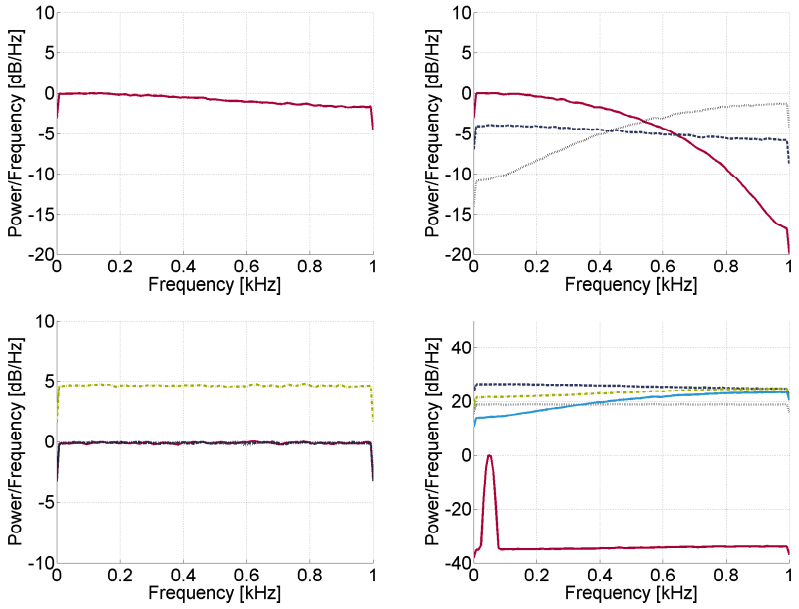

Figure 3.8: PSD estimates using simulated signals with three types of noise. Top,left - measured signal. Top, right - interfering noise 1 (red line), noise 2 (blue dashed line), noise 3 (gray dotted line). Bottom, left - measured noise 1 (red line), noise 2 (blue dashed line), noise 3 (gray dotted line) and total measured noise (green dashed line). Bottom, right - measured signal (blue dashed line), result after Wiener filtering with total interfering noise (gray dotted line), with noise 1 (green dashed line), with noise 1 and 2 (light blue line) and with noise 1, 2 and 3 (red line). See Figure 3.2 for details regarding the PSD settings.

3.3 ICA processing

The ICA processing will estimate the noise in the TAS signals. The noise estimate will then be used in the noise cancellation filters to enhance the contributions from the target, in this case the tones. The first question is which channels to include in the ICA processing. As mentioned previously two channels have been excluded as they showed a different spectrum in comparison to the remaining channels. It can be assumed that the self-noise originating from the towing ship should be more prominent in TAS elements which are located close to the towing ship. Furthermore, the self-noise originating from the hydrodynamic noise produced by the TAS in motion can be assumed to be

more or less uniformly distributed along all elements. Unfortunately there are no measurements without targets and neither is there any data which could reveal the self-noise dependence of the speed of the ship. Under these fairly weak assumptions and without having proper information regarding ambient- and self-noise characteristics, the 15 sensors closest to the ship were selected for ICA processing. Then the number of independent components has to be decided. As the data contained four tones, five independent components were searched for. The fifth component would in an ideal case mainly be composed of interfering noise. As five independent components are searched for, the five largest eigenvalues are kept in the whitening pre-processing of the signals. The ICA processing was tested on the signals, and in particular results will be presented for approximately 2.5 s of data taken from the starting phase of the measurement. In the optimisation five independent components were searched for, and the optimisation was stopped either if $\epsilon = 10^{-6}$, c.f. with $||\boldsymbol{w}_{new} \pm \boldsymbol{w}_{old}|| < \epsilon$ in Chapter 2, or if 1000 number of iterations was reached. The function $G_1(y)$ in equation 2.34 was used as the object function in the ICA processing.

In Figure 3.9, typical time signals after ICA processing are found for the present trial. The time signals in Figure 3.9 are normalised and four signals

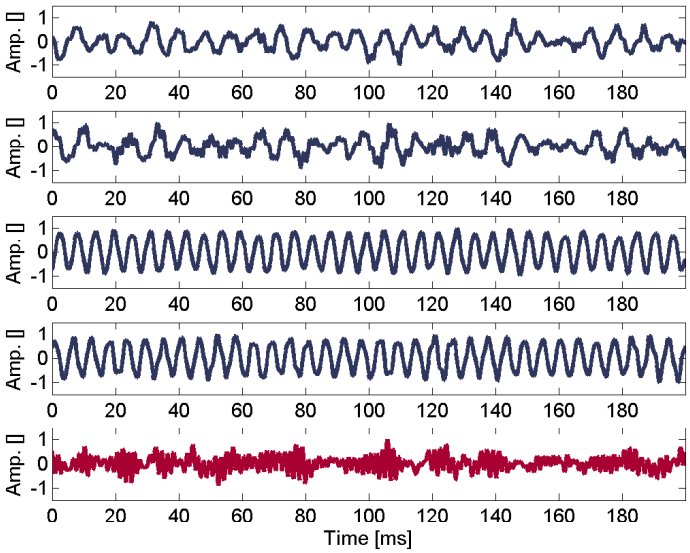

Figure 3.9: Normalised signal as function of time, corresponding to five independent components after ICA processing and using signals from 15 sensors. The four first signals show characteristics of tones (blue line), while the fifth has characteristics of noise (red line).

show characteristics of tones while the fifth has characteristics of noise. This becomes more evident when the corresponding normalised PSD estimates of the signals are considered, see Figure 3.10. The normalised PSD estimates have been calculated using approximately 2.5 s of data. In Figure 3.10, tones dominates in four spectra, while the fifth spectra has more characteristics of noise with a concentration of energy around 500 Hz.

The time signal with noise characteristics is then fed to the noise cancelation filters. The order of the filters were set to 200, 20, 20 and 10 for the

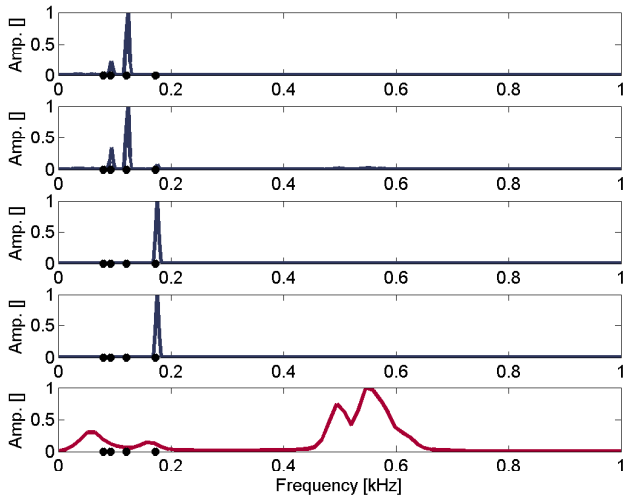

Figure 3.10: Normalised PSD estimates of time signals in Figure 3.9 using approximately 2.5 s of data. Estimates corresponds to five independent components after ICA processing and using signals from 15 sensors. The four first estimates show characteristics of tones (blue line), while the fifth has more broad band characteristics of noise (red line). Black dots indicate the frequencies of the tones. See Figure 3.2 for details regarding the PSD settings.

Wiener, LMS, NLMS and RLS filter respectively. The resulting PDS estimates using approximately 1.25 s of data from channel 30 are found in Figure 3.11, without and with filtering. As can be seen the reduction around 500 Hz is about 10 dB/Hz, which is as expected due to the noise signal fed to the filter having a concentration of energy around 500 Hz.

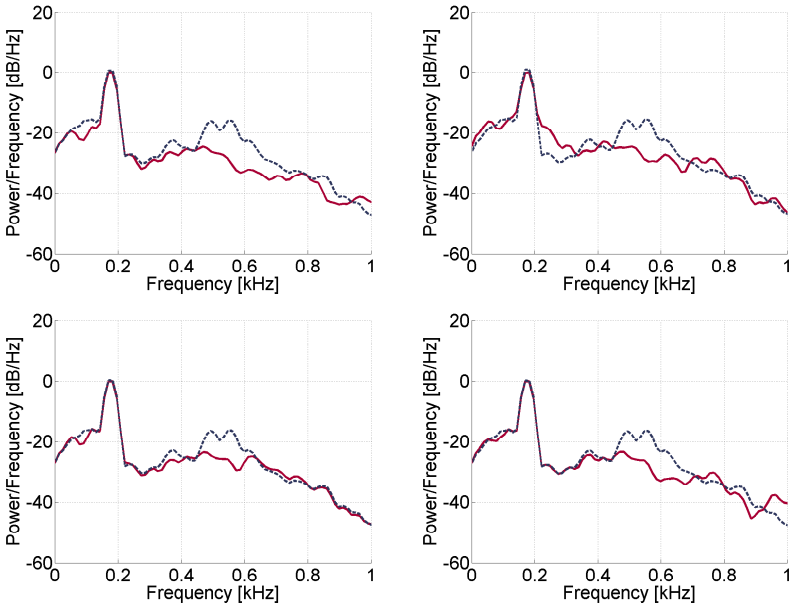

Figure 3.11: PDS estimates using approximately 1.25 s of data from channel 30 without (blue dashed line) and with filtering (red line). Wiener (top left), LMS (top right), NLMS (bottom left) and RLS (bottom right). See Figure 3.2 for details regarding the PSD settings.

4 Conclusions

Two promising self-noise cancellation methods have been applied to TAS signals from a field test carried out in the archipelago of Stockholm. Signals encompassed a target, four tones from a fixed source, and most likely additive self-noise and ambient noise. Unfortunately there were no measurements without targets establishing the properties of the ambient noise, neither was there any data which could reveal the self-noise dependence of the speed of the ship. Nevertheless, as the target consisted of tones, the discrimination of the target signal was simplified. Thus, the noise has to be estimated with the target present, which is a modification to the wanted prerequisites of the pre-processing when utilising the proposed methods.

The first combination of techniques consisted of an AR process which estimates the noise excluding only the tones from the target. This noise is then fed to the noise cancellation filters, Wiener, LMS, NLMS and RLS. This approach performed well on the measured signals and suppressed the noise at about 30 dB/Hz for all filters, even when the correlation coefficient between the corrupting and measured noise was very low. In the field test the SNR was high. Simulated data at low SNR was also investigated and in this case the noise was suppressed at about 60 dB/Hz.

The second combination of techniques, first estimates the noise by ICA. Signals were taken from the 15 sensors closest to the ship and then the dimension of the data was reduced to five by whitening. Thus, in the ICA processing five independent components were searched for, which produced four signals with characteristics of tones. The fifth signal could be attributed as noise with a concentration of energy in a frequency band not including the target tones. The ICA estimated noise signal was then fed to the noise cancellation filters. In the frequency band of the noise, a suppression at about 10 dB/Hz was achieved.

Results indicate that a reduction of self noise is obtained for simulated as well as real data sets, even when the self noise measurements have a low degree of correlation with the corrupting noise. Thus future research should be directed towards investigating an operational platform equipped with noise sensors. Alternatively the design of an onboard noise measurement system that can separately do self noise measurements with a reasonable degree of correlation should be investigated. In addition the spatial decorrelation effects arising from having the noise measurement system at different position than the sensor should be studied. Investigation of other methods to reduce the impact of self-noise without the need to separately measure the noise is of interest.

References

[1] M. Lasky, R.D. Doolittle, B.D. Simmons and S.G. Lemon. Recent progress in towed hydrophone array research. *IEEE Journal of Oceanic Engineering*, 29(2):374–387, 2004.

[2] R.J. Urick. *Principles of underwater sound.* McGraw-Hill, 1983.

[3] M.J. Hinich. Frequency-wavenumber array processing. *Journal of the Acoustical Society of America*, 69(3):732–737, 1981.

[4] C. Bao and D.C. Bertilone. Frequency-wavenumber analysis of self-noise in circular sonar arrays. In *Proceedings of Information, Decision and Control*, pages 235–240. Adelaide, Australia, 2002.

[5] G.R. Arrabito, B.E. Cooke and S.M. McFadden. Recommendations for enhancing the role of the auditory modality for processing sonar data. *Applied Acoustics*, 66:986–1005, 2005.

[6] I.S.D. Solomon and A.J. Knight. Spatial processing of signals received by platform mounted sonar. *IEEE Journal of Oceanic Engineering*, 27(1):57–65, 2002.

[7] T. Hoya, T. Tanaka, A. Cichocki, T. Murakami, G. Hori and J.A. Chambers. Stereophonic noise reduction using a combined sliding subspace projection and adpative signal enhancement. *IEEE Transactions on Speach and Audio Processing*, 13(3):309–320, 2005.

[8] C.-M. Kim, H.-M. Park, T. Kim, Y.-K. Choi and S.-Y. Lee. FPGA implementation of ICA algorithm for blind signal separation and adaptive noise canceling. *IEEE Transactions on Neural Networks*, 14(5):1038–1046, 2003.

[9] M.B. Priestley. *Spectral analysis and time series.* Academic Press, 1981.

[10] P. Common. Independent component analysis, a new concept? *Signal Processing*, 36:287–314, 1994.

[11] M.H. Hayes. *Statistical digital signal processing and modeling.* John Wiley, 1996.

[12] A. Hyvärinen. Fast and robust fixed-point algorithms for independent component analysis. *IEEE Transactions on Neural Networks*, 10(3):626–634, 1999.

[13] B. Widrow, J.R. Glover, J.M. McCool, J. Kaunitz, C.S. Williams, R.H. Heard, J.R. Zeidler, E. Dong and R.C. Goodlin. Adaptive noise cancelling: principles and applications. *Proceedings of the IEEE*, 63(12):1692–1716, 1975.

[14] J.J. Shynk. Adaptive IIR filtering. *IEEE Acoustics Speech Signal Processing Magazine*, 6(2):4–21, 1989.

[15] S.M. Kuo and D.R. Morgan. Active noise control: a tutorial review. *Proceedings of the IEEE*, 87(6):943–973, 1999.

[16] H. Lantz, E. Parastates, L. Persson and Ö. Staaf. Syntetisk aperturanalys av kabelsonardata. Technical Report FOI-R–0198–SE, Swedish Defence Research Agency, 2001.

[17] H.L. Van Trees . *Optimum array processing, part IV of detection, estimation, and modulation theory.* John Wiley, 2002.